COLLEGE OF ENGINEERING

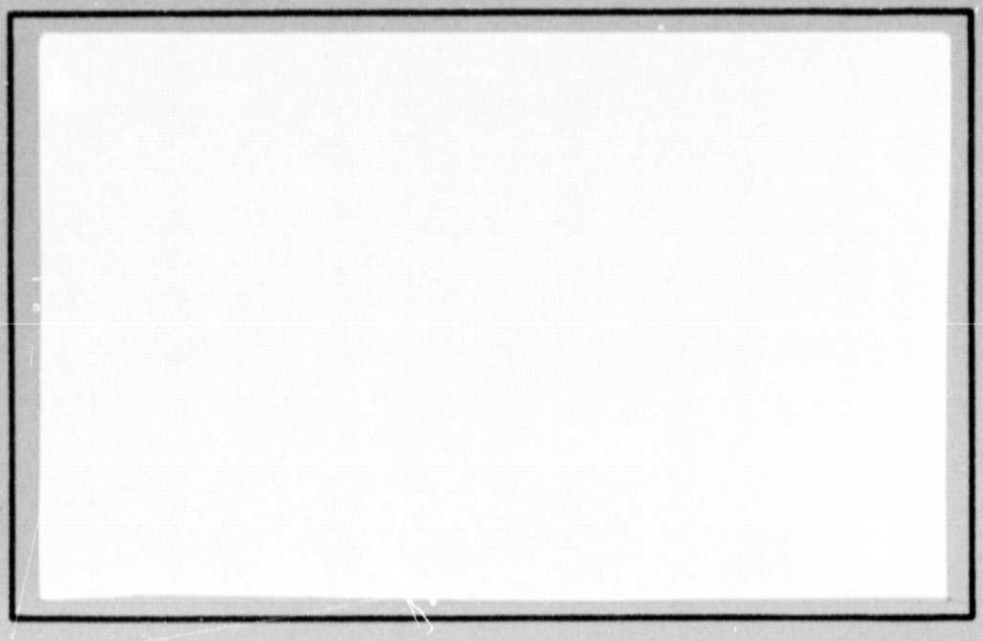

VIRGINIA POLYTECHNIC INSTITUTE AND STATE UNIVERSITY

BLACKSBURG, VIRGINIA

College of Engineering
Virginia Polytechnic Institute and State University
Blacksburg, VA 24061

VPI-E-79-9 February 1979

THE VISCOELASTIC BEHAVIOR OF THE PRINCIPAL COMPLIANCE MATRIX OF A UNIDIRECTIONAL GRAPHITE/EPOXY COMPOSITE

by

D. H. Morris[1], Y. T. Yeow[2], and H. F. Brinson[1]

[1] Department of Engineering Science and Mechanics
Virginia Polytechnic Institute and State University
Blacksburg, VA 24061

[2] Allied Chemical Corp.
Morristown, NJ 07960

Prepared for:

National Aeronautics and Space Administration
Grant No. NASA-NSG 2038
Materials and Physical Sciences Branch
Ames Research Center
Moffett Field, CA 94035

ABSTRACT

A testing program was conducted to determine the time-temperature response of the principal compliances of a unidirectional graphite/epoxy composite. It is shown that two components of the compliance matrix are time and temperature independent. In addition, the compliance matrix is found to be symmetric for the viscoelastic composite.

The time-temperature superposition principle is used to determine shift factors. It is shown that shift factors are independent of fiber orientation, for fiber angles that vary from 10° to 90° with respect to the load direction.

TABLE OF CONTENTS

LIST OF TABLES

LIST OF FIGURES

INTRODUCTION

Composite materials are finding increasing use in the aerospace and automotive industries. These materials may exhibit time-dependent mechanical behavior, depending upon the state of stress, temperature, and relative humidity [1]. Thus, it is necessary to measure the time-dependent effects if the materials are to be used for structural applications. That such time dependent effects are important has been previously demonstrated [2]. The result is shown in Fig. 1, which indicates that a delayed viscoelastic fracture process was observed for a graphite/epoxy $[\pm 45]_{4s}$ tensile specimen containing a circular hole. That is, the laminate eventually fractured even though the applied load was relaxing in a fixed grip situation. The reason this is possible is directly related to the construction of the laminated composite being tested. That is, cracks can open and propagate in one ply leading to creep within that ply. This in turn leads to a transfer of load to adjacent plies. Thus, while the overall laminate may be relaxing, individual fractured plies may exhibit a creep response. Obviously, should the same phenomena occur in a prototype structure, premature failures would occur.

It would be desirable to measure the time-dependent effects with short-term laboratory tests rather than perform long-term prototype studies. It is then clear that there is a need for accelerated characterization techniques for composite laminates similar to those used for other structural materials.

For metals and polymers a variety of accelerated characterization techniques are available such as linear elastic stress analysis, empirical extrapolative equations such as the Larson-Miller parameter method, Minor's rule and frequency independence, the time-temperature superposition principle, etc. The approach taken in the work reported herein is based upon the time-temperature superposition principle developed for polymeric materials, and the widely used lamination theory developed for composite materials.

The procedures for accelerated characterization and lifetime prediction are outlined in Figs. 2 and 3. Figure 2 illustrates the plan to determine the modulus master curve for unidirectional laminates from short-term (15 min.) tensile creep tests from room temperature to about 30°C above the glass transition temperature (180°C). Testing should occur for various fiber angles from 0° to 90° with respect to the load direction. From this series of tests shift functions versus temperature and fiber angle are to be determined, as shown in Fig. 2b. Linear viscoelasticity will be assumed, and lamina tensile and shear strength master curves will be obtained by assuming that a strength master curve has the same character as a modulus master curve.

Probably the most important aspect of the accelerated characterization plan is the generation of a shift function relation, such as shown in Fig. 2d. A more detailed discussion of the shift function relation will be given later.

The authors envision the final accelerated design process as illustrated by the flow chart shown in Fig. 3. The success of the plan shown in Fig. 3 is dependent upon several assumptions. Two critical

assumptions occur in boxes B and F of the flow chart of Fig. 3. These assumptions involve symmetry of the principal compliance matrix used in modulus transformation equations (box B), and equality of shift function with fiber angle (box F). The major thrust of the remainder of this paper is directed toward a critical analysis of the two assumptions. Once the assumptions are proved valid, then the remaining portion of the plan shown in Fig. 3 should follow and be reasonably accurate.

In order to see how the assumptions fit into the flow chart of Fig. 3, it is first necessary to establish the constitutive theory for a lamina. Assuming a state of plane stress in an orthotropic material, the constitutive equation may be written [3],

$$\begin{bmatrix} \epsilon_x \\ \epsilon_y \\ \gamma_{xy} \end{bmatrix} = \begin{bmatrix} S'_{11} & S'_{12} & S'_{16} \\ S'_{12} & S'_{22} & S'_{26} \\ S'_{16} & S'_{26} & S'_{66} \end{bmatrix} \begin{bmatrix} \sigma_x \\ \sigma_y \\ \tau_{xy} \end{bmatrix} \tag{1}$$

where the x-y coordinate system is as shown in Fig. 4. If the coordinate system is aligned with the lamina principal axes 1-2 (1 denotes the fiber direction and 2 denotes the normal to the fiber direction), Eq. (1) becomes

$$\begin{bmatrix} \epsilon_1 \\ \epsilon_2 \\ \gamma_{12} \end{bmatrix} = \begin{bmatrix} S_{11} & S_{12} & 0 \\ S_{12} & S_{22} & 0 \\ 0 & 0 & S_{66} \end{bmatrix} \begin{bmatrix} \sigma_1 \\ \sigma_2 \\ \tau_{12} \end{bmatrix} \tag{2}$$

In Eqs. (1) and (2) the S'_{ij} and S_{ij} are compliance matrices and are related through tensor transformation equations [3]. For example,

$$S'_{11} = m^4 S_{11} + 2m^2 n^2 S_{12} + n^4 S_{22} + m^2 n^2 S_{66} \qquad (3)$$

where $m = \cos\theta$ and $n = \sin\theta$ (see Fig. 4). Similar relations exist between other components of the compliance matrices [3]. All primed quantities are only a function of the four principal compliances of Eq. (2) and the angle θ.

Thus, one need only determine the principal compliances from Eq. (2) to completely define the state of stress or strain for a continuous fiber reinforced composite under a state of plane stress. If the material is viscoelastic, the components of the principal compliance matrix will be a function of time, temperature, relative humidity, and stress level [1,4,5]. The present study will consider stress levels such that material response is linear viscoelastic. In addition, relative humidity will not be an experimental variable.

When the composite material response is linear viscoelastic, Eq. (3) may be written [5]

$$S'_{11}(t) = m^4 S_{11}(t) + 2m^2 n^2 S_{12}(t) + n^4 S_{22}(t) + m^2 n^2 S_{66}(t) \qquad (4)$$

where t denotes time. Equation (4), together with composite lamination theory, may be used to predict the viscoelastic behavior of a general laminate.

In brief, the plan consists of constructing master compliance curves for unidirectional laminates from short-term creep tests at various temperatures. This requires the use of the time-temperature superposition principle. From the short-term tests the shift function versus temperature relationship may also be found. Using the master compliance curves, the shift functions, and equations similar to

Eq. (4), compliance master curves for any angle θ (Fig. 4) could be constructed. These master curves could then be used as input to an incremental computational procedure using standard stress analysis lamination theory to predict long-term material behavior.

As previously mentioned the above procedure is dependent upon the use of transformation equations, such as Eq. (4), and the shift function-temperature relationship. Two comments are in order regarding the previous statement. First, in writing Eq. (4) it is assumed that the compliance matrix in Eq. (2) is symmetric, that is, $S_{12}(t) = S_{21}(t)$. And second, for Eq. (4) to be of practical use, the shift functions for the components of the principal compliance matrix, Eq. (2), should be equal.

Based on these comments, the objective of this paper is twofold; (1) check the assumption that $S_{12}(t) = S_{21}(t)$, and (2) show whether the shift function-temperature relationship is the same for various angles θ, that is, show whether the shift function is independent of fiber orientation.

EXPERIMENTAL CONSIDERATIONS

The particular composite material studied in this investigation was manufactured from T300/934 graphite/epoxy pre-preg tapes. All test specimens were cut from a single large panel of the material. In addition, all specimens were unidirectional laminates.

Tensile specimens were instrumented with three-element rectangular strain gage rosettes. Two rosettes were bonded to each specimen, one on each side, and the gage outputs were averaged to eliminate any

out-of-plane bending. The strain gage rosettes were temperature compensated using specimens whose fiber orientation was identical to the stressed specimens.

Load was applied to test specimens through special grips, similar to those used by Chamis and Sinclair [6]. They show that these grips, together with the specimen length used, tended to minimize the in-plane bending discussed by Pagano and Halpin [7]. The grips used by Chamis and Sinclair were modified by the addition of a pin that extended through the midpoint of the clamped specimen section. This pin helped to reduce slippage between the metal clamps, bonded end tabs, and test specimen. Load levels were such that material response was always linear viscoelastic. Further discussion of the experimental procedures may be found elsewhere [8].

ANALYTICAL CONSIDERATIONS

As previously stated, one can completely characterize lamina viscoelastic behavior by determining the principal compliances $S_{11}(t)$, $S_{22}(t)$, $S_{12}(t)$, and $S_{66}(t)$ that appear in Eq. (4). Thus, in order to answer the questions raised in the objective statement, it is appropriate to discuss the methods whereby the components of the principal compliance matrix were determined.

First, let $\theta = 0$ (Fig. 4) and write the principal compliance $S_{11}(t)$ as

$$S_{11}(t) = \frac{e_1(t)}{\sigma_o} \tag{5}$$

where $e_1(t)$ denotes that the axial strain is a function of time, and

σ_o is the constant applied stress. The axial component of strain (as well as those that follow) was found using the strain gage rosettes. A creep test of the same specimen simultaneously yielded the value of $S_{12}(t)$ from the expression

$$S_{12}(t) = \frac{\epsilon_2(t)}{\sigma_o} \tag{6}$$

where $\epsilon_2(t)$ is the time dependent transverse strain.

In order to check the assumption of symmetry of the principal compliance matrix, it is necessary to experimentally determine $S_{21}(t)$ from

$$S_{21}(t) = \frac{\epsilon_1(t)}{\sigma_o} \tag{7}$$

where $\theta = 90°$ in Fig. 4. Note that $\epsilon_1(t)$ does not have the same meaning in Eqs. (5) and (7).

The two remaining principal compliances are found as follows. Letting $\theta = 90°$, the compliance $S_{22}(t)$ may be written as

$$S_{22}(t) = \frac{\epsilon_2(t)}{\sigma_o} \tag{8}$$

where $\epsilon_2(t)$ is the time dependent axial strain. The compliance $S_{66}(t)$ was found using

$$S_{66}(t) = \frac{\gamma_{12}(t)}{\tau_{12}} \tag{9}$$

where $\theta = 10°$. Further discussion on the applicability of Eq. (9) for calculating $S_{66}(t)$ may be found in Ref. [8]. In Eq. (9), τ_{12} is a constant intralaminar shear stress and is found via the stress

transformation equation

$$\tau_{12} = \frac{1}{2} \sigma_o \sin 2\theta \tag{10}$$

The time dependent shear strain, $\gamma_{12}(t)$, is determined from the strain transformation equation

$$\gamma_{12} = - (\epsilon_x - \epsilon_y) \sin 2\theta + \gamma_{xy} \cos 2\theta \tag{11}$$

where

$$\gamma_{xy} = 2\epsilon_{45} - \epsilon_x - \epsilon_y \tag{12}$$

In Eqs. (11) and (12), ϵ_x, ϵ_y and ϵ_{45} are the axial, transverse and 45° strains, respectively, obtained from the three-element rectangular strain gage rosettes.

Equations (5) - (12) may be used to evaluate the components of the principal compliance matrix. In particular, Eqs. (6) and (7) may be used to determine the symmetry of the compliance matrix. Using Eqs. (5), (6), (8), and (9) and short-term experimental results, one can construct master compliance curves and find shift functions, and thus determine whether the shift functions are independent of fiber orientation, θ.

RESULTS AND DISCUSSION

Symmetry of Compliance Matrix

Table 1 shows the experimental results for $S_{12}(t)$ and $S_{21}(t)$, for t = 1 min. Similar results were found for other values of time up to 15 min., which was the extent of the short-term tests. Several results are evident from inspection of the data in Table 1. Both S_{12}

and S_{21} are essentially independent of temperature (within about 10%). The maximum temperature was 210°C. Data at t = 15 min. indicated that S_{12} and S_{21} are within about 10% of the values of Table 1, which shows that these compliance terms are also essentially independent of time. The average values of S_{12} and S_{21} in Table 1 are within 9% of each other. The differences cited above are probably due to experimental error due to the small transverse strains measured in a $\theta = 90°$ test, and due to the fact that only one test was conducted at each temperature level. It is felt that the scatter in data represents usual variations in test results encountered in composite materials. Henceforth, the compliance matrix will be considered symmetric. In addition, it will be assumed that S_{12} is independent of time and temperature. Experimental results also indicate that S_{11} is independent of time and temperature. Similar results have been found for a unidirectional glass fiber-epoxy composite material [1].

Equality of Shift Functions

Before proceeding with a discussion of the equality of shift functions, it is appropriate to briefly discuss the methods whereby the results were obtained. Further details may be found in [9].

Figure 5 illustrates the time-temperature behavior of the reduced reciprocal of S_{66} ($\theta = 10°$), for short-term (15 min.) creep. The reduced compliance was calculated from

$$S_{66}(t) = \frac{\epsilon_2(t)}{\sigma_o} \frac{T}{T_o} \tag{13}$$

where T represents the absolute test temperature and T_o was the absolute

reference temperature (taken as the glass transition temperature of 453°K, [8]). The ordinate of Fig. 5 was plotted in terms of reduced reciprocal of compliance in order to study the applicability of the time-temperature superposition principle to composite materials [8,9]. Figure 5 also shows a portion of the master curve at the reference temperature of 453°K, or 180°C. A complete master curve was obtained by graphically shifting the short-term curves along the log time axis until one continuous curve was obtained. The shift factor was the amount of horizontal shifting necessary to superpose the various constant temperature curves.

Figure 6 shows shift factors, a_T, for fiber orientations that range from 10° to 90°. For fiber orientations of 15°, 30°, 45°, 60°, and 75°, compliances were calculated using an equation similar to Eq. (9), and Eqs. (10), (11), and (12). For all practical purposes the shift factors in Fig. 6 are equal, and thus are independent of fiber orientation. A similar result has been found by Moehlenpah, Ishai, and DiBenedetto [10] for the tensile yield stress shift factors for glass fiber reinforced epoxies. Note that S_{11} and S_{12} are independent of time and temperature and do not require the use of shift functions.

As seen in Fig. 6, there is scatter in experimental data. However, above the glass transition temperature of 180°C data scatter is slight. Some of the reasons for scatter, or lack thereof, may be seen by examination of Fig. 5. Above 180°C the slopes of the compliance-time curves are greater than for temperatures less than 180°C. Thus, graphical shifting was more accurate for temperatures above the glass transition temperature. In addition, as previously stated, only one

test was conducted at each temperature level. It is felt that the data scatter is typical of that found when testing composite materials. For more accurate results several tests at a particular temperature should be conducted.

CONCLUSIONS

It has been shown that the principal compliance matrix for an orthotropic body under plane stress is symmetric. Two components of the matrix, S_{11} and S_{12}, are time and temperature independent. Similar results have been found for a glass-epoxy unidirectional composite [1]. In addition, shift factors are independent of fiber orientation for fibers oriented between 10° and 90° to the load direction.

Both of the above results are important when using the tensor transformation equations to predict the time-dependent compliant behavior of off-axis unidirectional laminates, and hence general laminate behavior as shown in the plan of Fig. 3.

Obviously, if reliable values of principal compliances, master curves, and shift factors are to be obtained, then many tests will be needed to establish the statistical variation of properties with time and temperature. That was not the purpose of the work reported herein.

ACKNOWLEDGMENTS

The financial support provided for this work by NASA Grant NSG 2038 from the Materials and Physical Sciences Branch of Ames Research Center is gratefully acknowledged. Further, sincere appreciation is extended to H. G. Nelson and D. P. Williams of NASA-Ames for their encouragement and many helpful suggestions.

REFERENCES

1. Y. C. Lou and R. A. Schapery, "Viscoelastic Characterization of a Nonlinear Fiber-Reinforced Plastic," Journal of Composite Materials, Vol. 5, April 1971, pp. 208-234.

2. Y. T. Yeow and H. F. Brinson, "A Study of Damage Zones or Characteristic Lengths as Related to the Fracture Behavior of Graphite/Epoxy Laminates," Virginia Polytechnic Institute and State University, VPI-E-77-15, May 1977.

3. R. M. Jones, Mechanics of Composite Materials, McGraw-Hill Book Co., New York, 1975.

4. J. C. Halpin, "Introduction to Viscoelasticity," in Composite Materials Workshop, S. W. Tsai, J. C. Halpin, and N. J. Pagano, Eds., Technomic Publishing Co., 1968.

5. J. C. Halpin and N. J. Pagano, "Observations on Linear Anisotropic Viscoelasticity," Journal of Composite Materials, Vol. 2, Jan. 1968, pp. 68-80.

6. C. C. Chamis and J. H. Sinclair, "Ten-Deg. Off-Axis Tensile Test for Intralaminar Shear Characterization of Fiber Composites," NASA TN D-8215, 1976.

7. N. J. Pagano and J. C. Halpin, "Influence of End Constraints in the Testing of Anisotropic Bodies," Journal of Composite Materials, Vol. 2, Jan. 1968, pp. 18-31.

8. Y. T. Yeow, D. H. Morris and H. F. Brinson, "The Time-Temperature Behavior of a Unidirectional Graphite/Epoxy Composite," Composite Materials: Testing and Design (Fifth Conference), ASTM STP 674, 1979 (in press).

9. Y. T. Yeow, "The Time-Temperature Behavior of Graphite Epoxy Laminates," Ph.D. Dissertation, Virginia Polytechnic Institute and State University, Blacksburg, VA, May 1978.

10. A. E. Moehlenpah, O. Ishai and A. T. DiBenedetto, "The Effect of Time and Temperature on the Mechanical Behavior of Epoxy Composites," Polymer Engineering and Science, Vol. 11, March 1971, pp. 129-138.

Table 1. Measured Properties S_{12} and S_{21} (1 min.) for T300/934 Graphite/Epoxy Composite.

Temperature (°C)	$S_{12} \times 10^6$ psi^{-1} ($\times 10^4$ MPa^{-1})	$S_{21} \times 10^6$ psi^{-1} ($\times 10^4$ MPa^{-1})
22	-0.0149 (-0.0216)	-0.0143 (-0.0207)
100	-0.0124 (-0.0180)	-0.0148 (-0.0215)
180	-0.0132 (-0.0191)	-0.0144 (-0.0209)
200	-0.0140 (-0.0203)	-0.0147 (-0.0213)
210	-0.0136 (-0.0197)	-0.0157 (-0.0228)

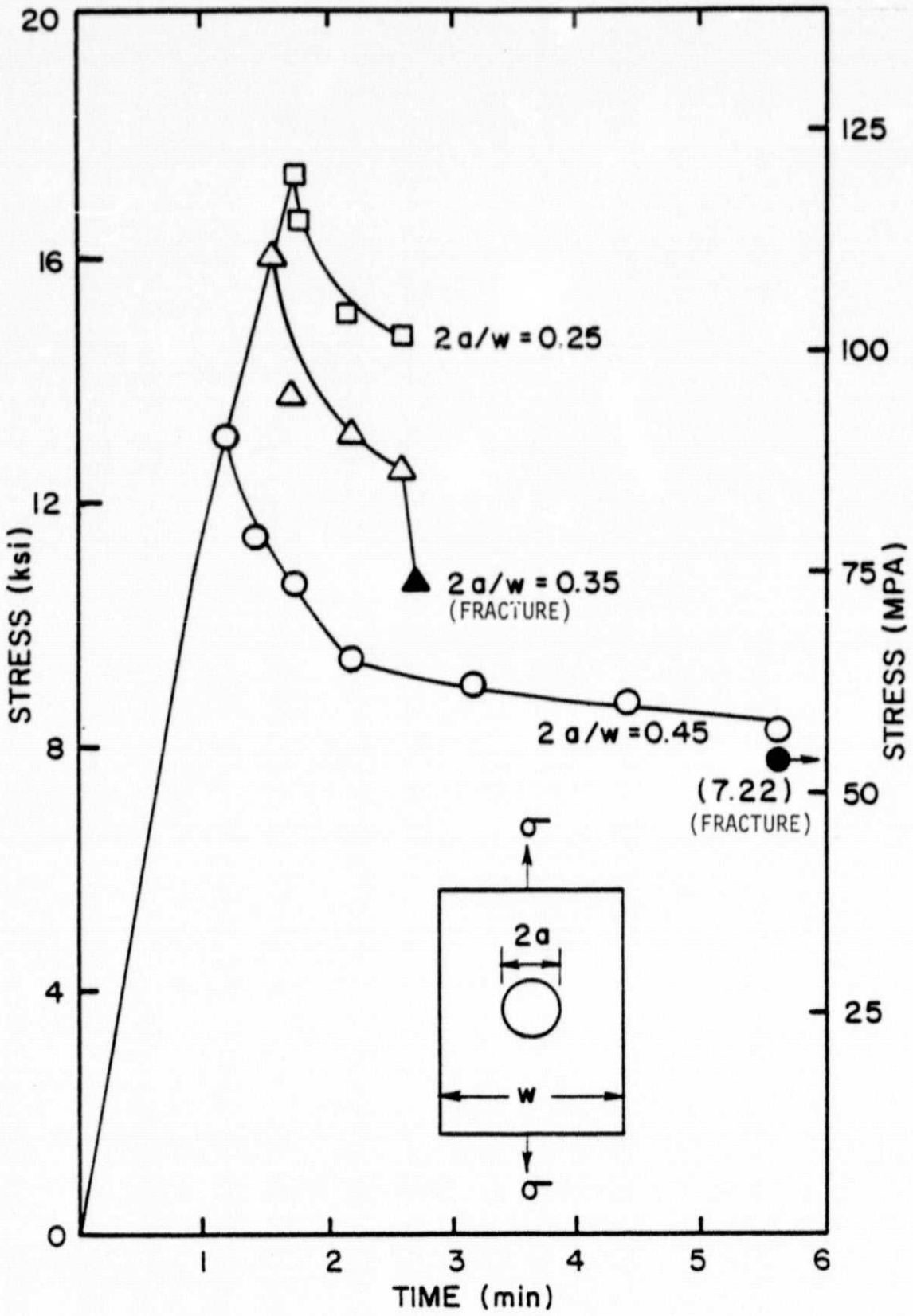

Fig. 1. Time-Dependent Fracture of $[\pm 45]_{4s}$ T300/934 Graphite/Epoxy Plate With a Central Circular Hole

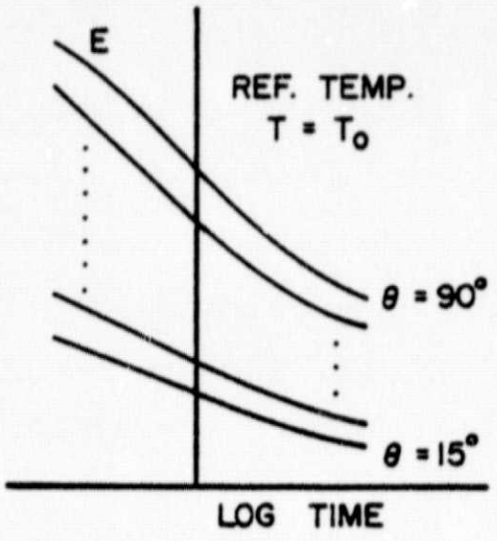

a) MEASURED TENSILE MODULUS MASTER CURVES VS. FIBER ANGLE FOR UNIDIRECTIONAL LAMINATE.

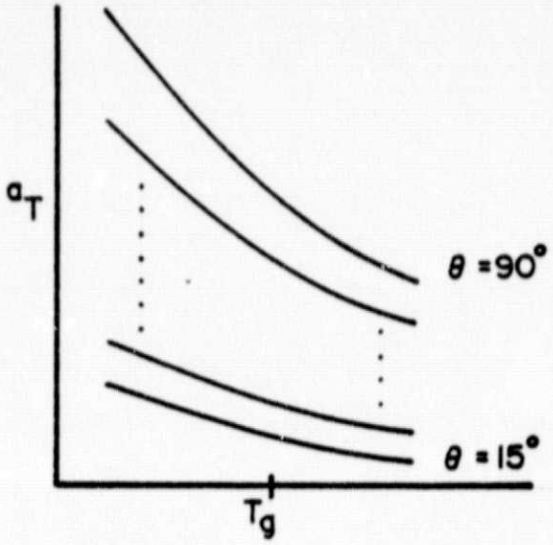

b) MEASURED SHIFT FUNCTION VS. FIBER ANGLE FOR UNIDIRECTIONAL LAMINATE.

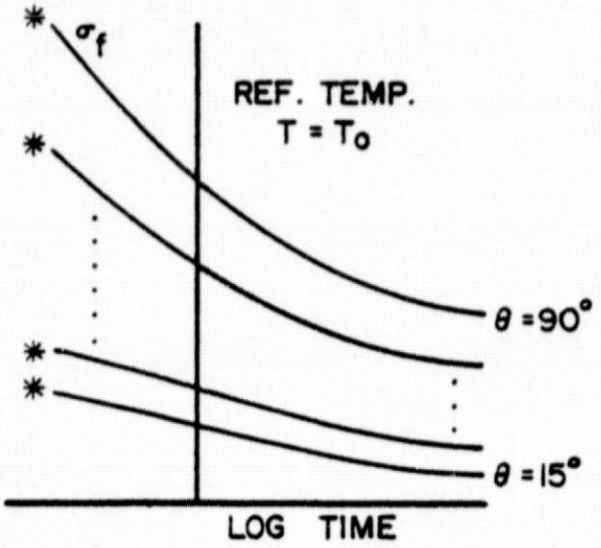

c) TENSILE STRENGTH MASTER CURVE ASSUMED TO HAVE SAME CHARACTER AND SHIFT FUNCTION AS MODULUS MASTER CURVE (*MEASURED DATA).

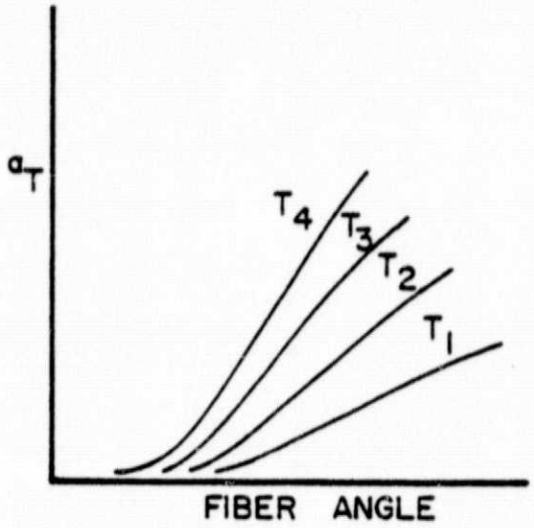

d) FORMAL SHIFT FUNCTION VS. FIBER ANGLE AND TEMPERATURE RELATION ANALOGOUS TO WFL EQUATION DEVELOPED FROM b).

Fig. 2. Proposed Method to Determine Tensile Strength Master Curve and Shift Function Equation

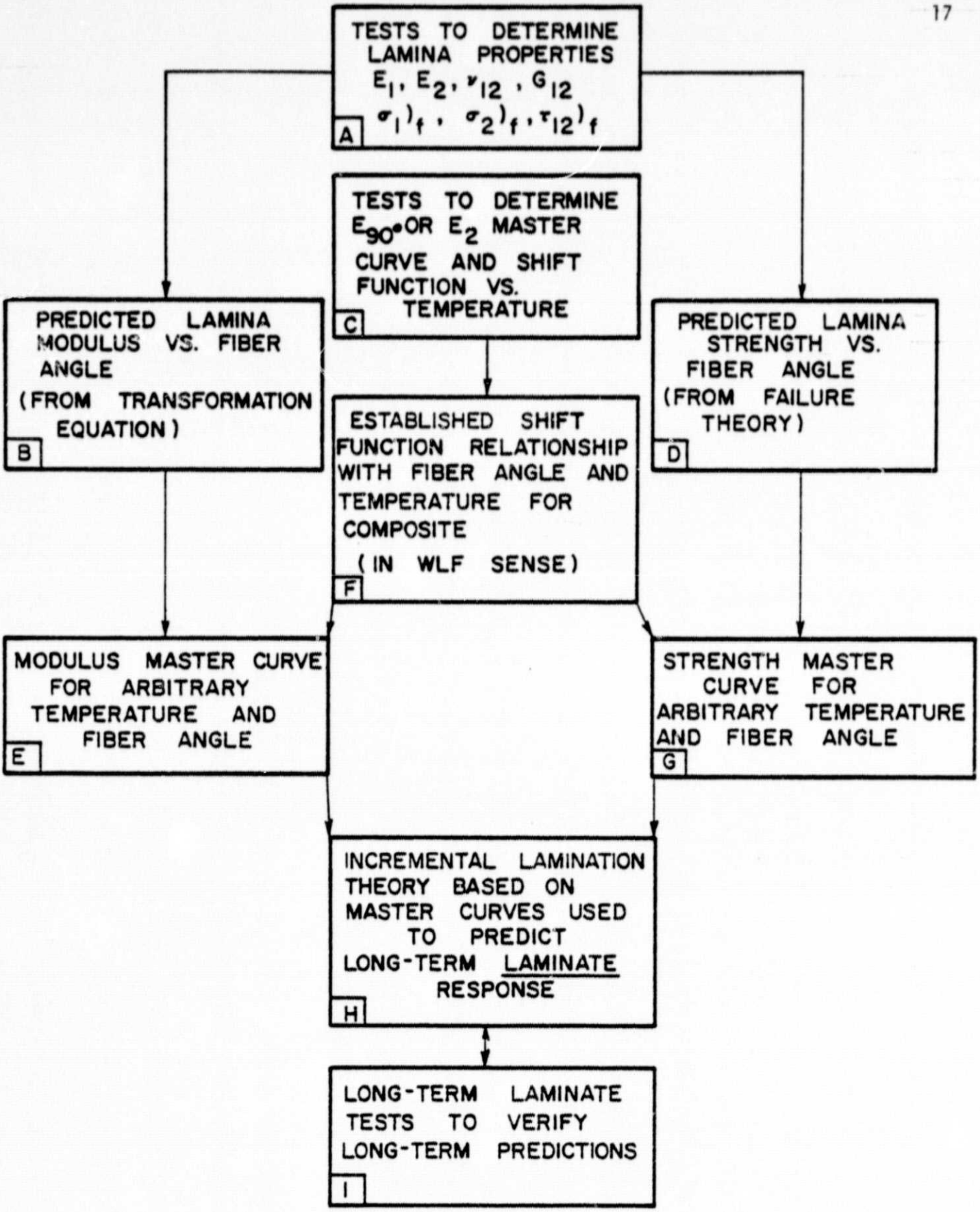

Fig. 3. Flow Chart of the Proposed Procedures for Laminate Accelerated Characterization and Failure Prediction

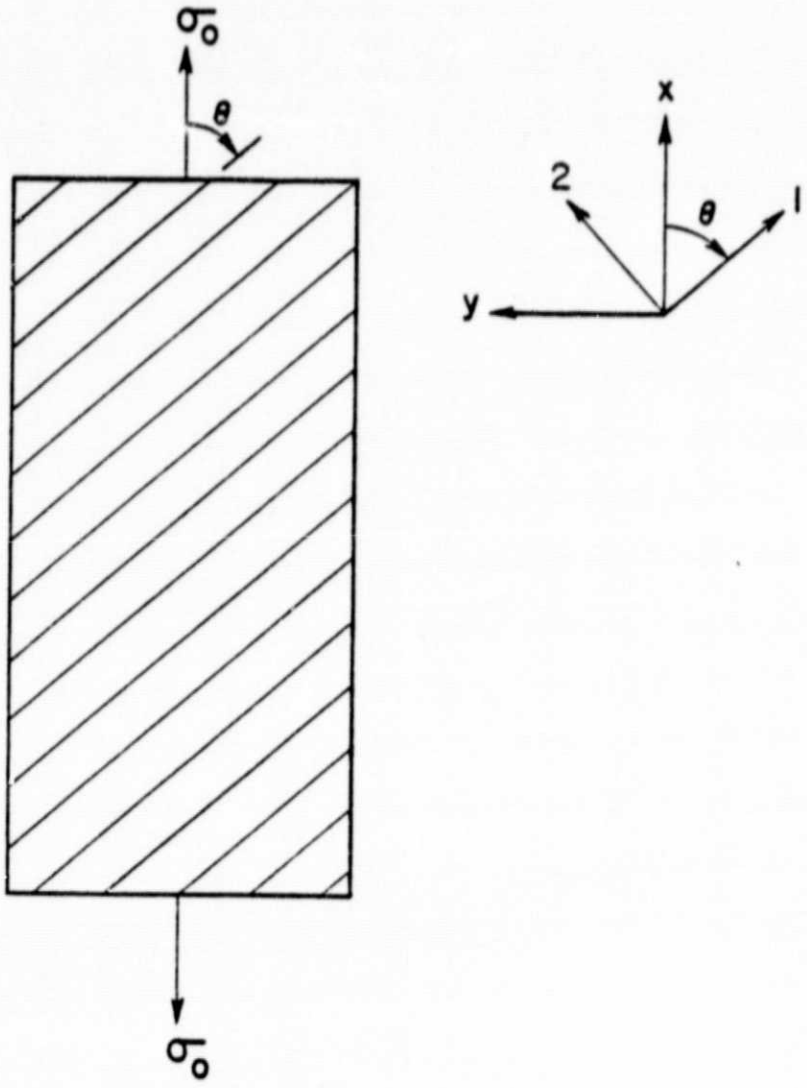

F.g. 4. Schematic of Off-Axis Tensile Coupon

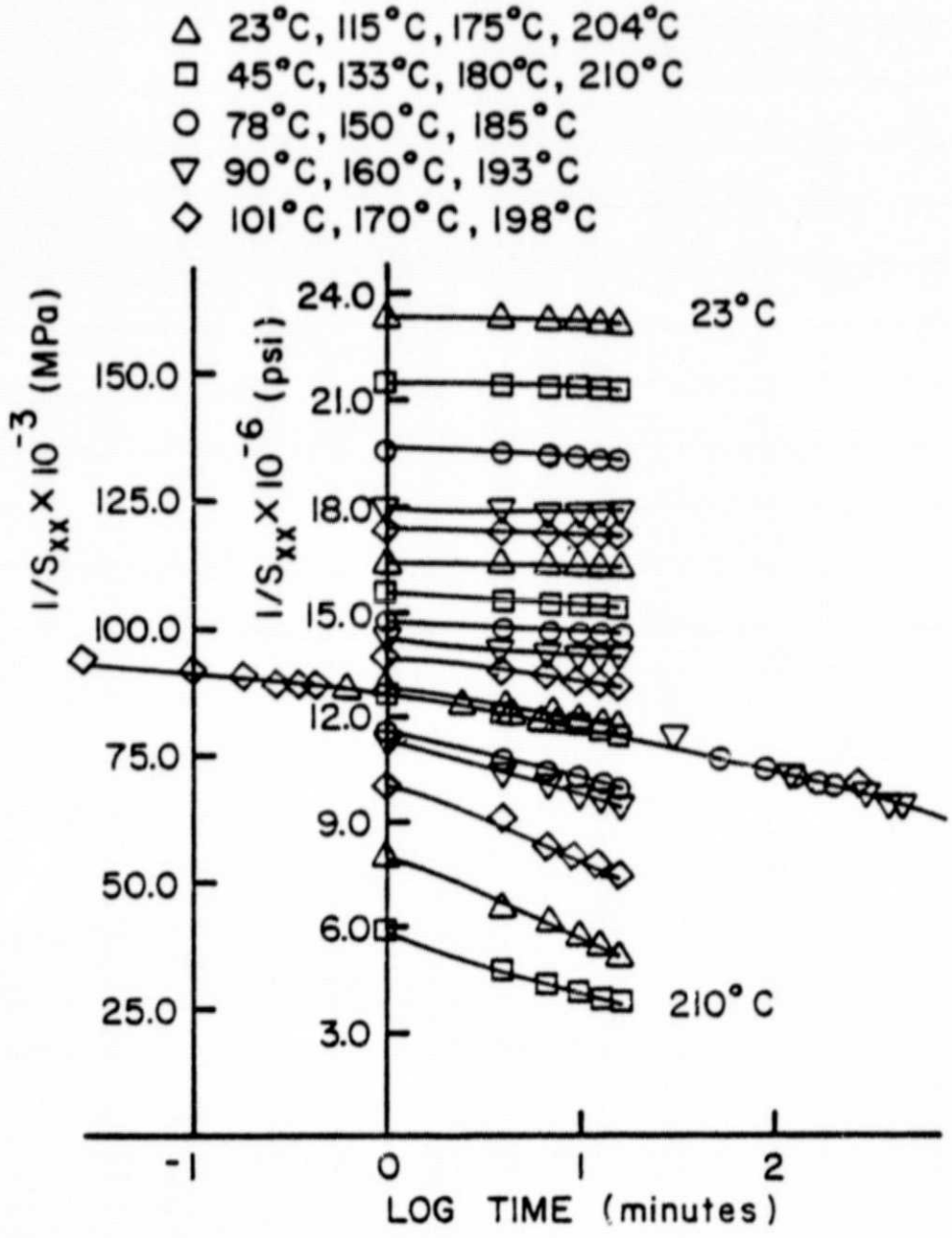

Fig. 5. Reduced Reciprocal of Compliance and Portion of 180°C Master Curve for $[10°]_{8s}$ T300/934 Graphite/Epoxy Laminate

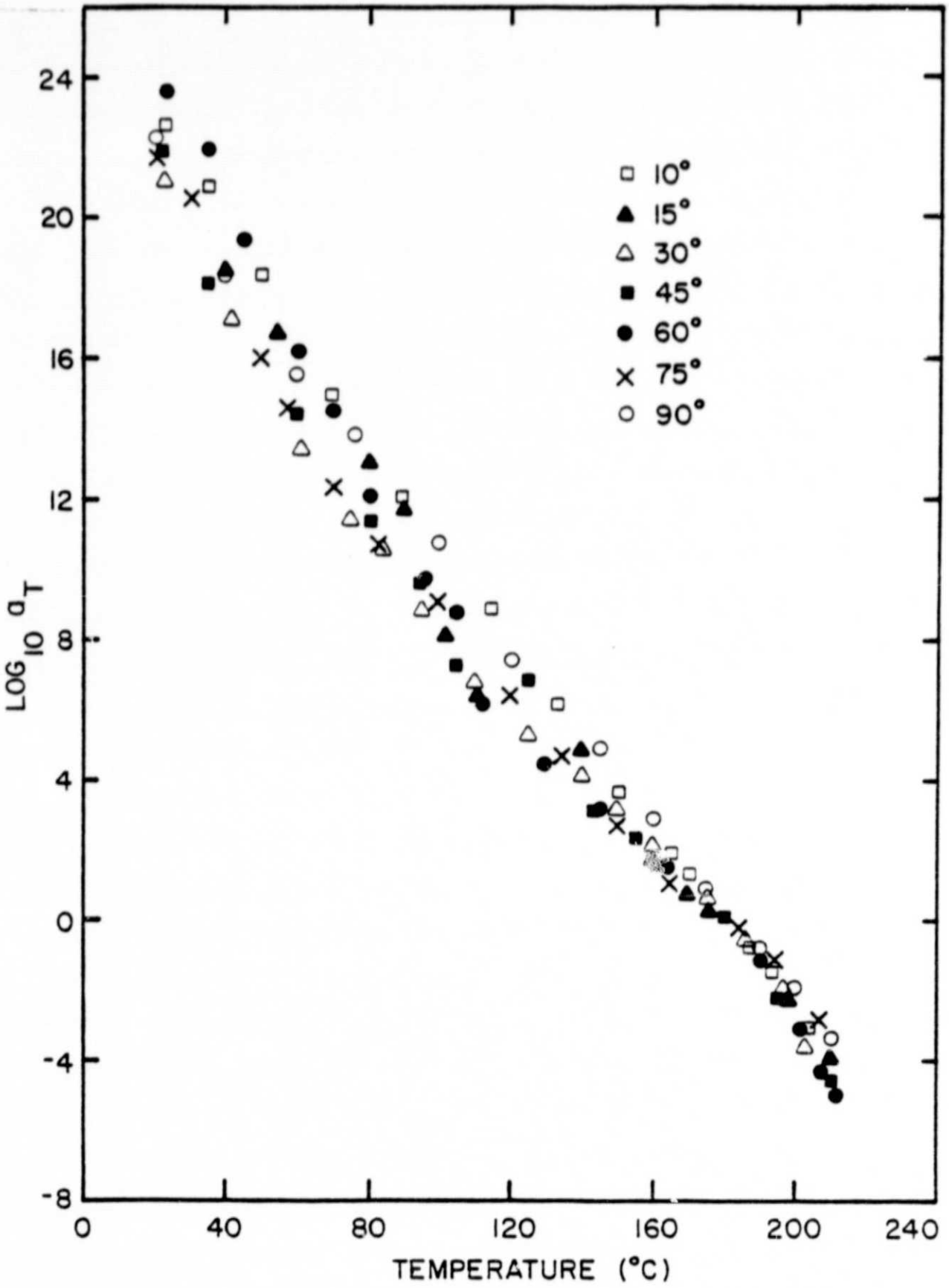

Fig. 6. Shift Factors versus Temperature for Creep of Off-Axis Tensile Coupons (T300/934 Graphite/Epoxy)